Published in final edited form as:
J Microbiol Methods. 2014 January ; 96: 104–110. doi:10.1016/j.mimet.2013.11.010.

Developmental transitions of *Coxiella burnetii* grown in axenic media

Kelsi M. Sandoz[1], **Daniel E. Sturdevant**[2], **Bryan Hansen**[3], and **Robert A. Heinzen**[1,*]

[1]*Coxiella* Pathogenesis Section, Laboratory of Intracellular Parasites, Rocky Mountain Laboratories, National Institute of Allergy and Infectious Diseases, National Institutes of Health, Hamilton, MT 59840

[2]Genomics Unit, Research Technologies Branch, Rocky Mountain Laboratories, National Institute of Allergy and Infectious Diseases, National Institutes of Health, Hamilton, MT 59840

[3]Electron Microscopy Unit, Research Technologies Branch, Rocky Mountain Laboratories, National Institute of Allergy and Infectious Diseases, National Institutes of Health, Hamilton, MT 59840

Abstract

Coxiella burnetii undergoes a biphasic developmental cycle within its host cell that generates morphologically and physiologically distinct large cell variants (LCV) and small cell variants (SCV). During the lag phase of the *C. burnetii* growth cycle, non-replicating SCV differentiate into replicating LCV that in turn differentiate back into SCV during stationary phase. Nearly homogeneous SCV are observed in infected Vero cells after extended incubation (21 to 28 days). In the current study, we sought to establish whether *C. burnetii* developmental transitions in host cells are recapitulated during host cell-free (axenic) growth in first and second generation acidified citrate cysteine media (ACCM-1 and ACCM-2, respectively). We show that ACCM-2 supported developmental transitions and viability. Although ACCM-1 also supported SCV to LCV transition, LCV to SCV transition did not occur after extended incubation (21 days). Instead, *C. burnetii* exhibited a ghost-like appearance with bacteria containing condensed chromatin but otherwise devoid of cytoplasmic content. This phenotype correlated with a near total loss in viability between 14 and 21 days of cultivation. Transcriptional profiling of *C. burnetii* following 14 days of incubation revealed elevated expression of oxidative stress genes in ACCM-1 cultivated bacteria. ACCM-2 differs from ACCM-1 by the substitution of methyl-β-cyclodextrin (Mβ-CD) for fetal bovine serum. Addition of Mβ-CD to ACCM-1 at 7 days post-inoculation rescued *C. burnetii* viability and lowered expression of oxidative stress genes. Thus, Mβ-CD appears to alleviate oxidative stress in ACCM-2 to result in *C. burnetii* developmental transitions and viability that mimic host cell-cultivated organisms. Axenic cultivation of *C. burnetii* in ACCM-2 and new methods of genetic manipulation now allow investigation of the molecular basis of *C. burnetii* biphasic development.

Keywords

Q fever; *Coxiella*; differentiation; axenic growth; development; viability

[*]To whom correspondence should be addressed: Mailing address: Rocky Mountain Laboratories, 903 South 4th Street, Hamilton, Montana 59840. Phone: (406) 375-9695. Fax: (406) 363-9380. rheinzen@niaid.nih.gov.

1. Introduction

Coxiella burnetii is a zoonotic bacterial pathogen that causes a disease in humans called Q fever. Acute disease normally presents as a self-limited, incapacitating influenza-like illness. Less frequent but more serious is chronic Q fever that generally manifests as endocarditis. Transmission to humans is facilitated by *C. burnetii*'s high infectivity and aerosol route of infection. Sheep, goats, and dairy cattle are important animal reservoirs that can deposit tremendous numbers of organisms into the environment during parturition. Exposure to contaminated aerosols generated by animal husbandry operations can consequently result in Q fever outbreaks, as recently observed in the Netherlands where the largest disease outbreak on record (> 4,000 cases) occurred in association with high-density dairy goat farming (Huijsmans et al., 2011, Roest et al., 2011).

C. burnetii is an intracellular pathogen that has a tropism for mononuclear phagocytes during infection. Following internalization, the bacterium replicates in a vacuole with phagolysosomal characteristics (Voth and Heinzen, 2007). Resistance to lysosomal digestion is associated with remarkable environmental stability, a characteristic that contributes to disease transmission. The pathogen is highly resistant to osmotic shock, elevated temperature, desiccation, ultraviolet light, and various chemical disinfectants (McCaul et al., 1981, Williams, 1991), and can remain infectious in barnyard dust for weeks to months (Tissot-Dupont et al., 2004). The spore-like characteristics of *C. burnetii* are speculated to reside with a stable small cell variant (SCV) that arises as part of a biphasic developmental cycle (Heinzen et al., 1999, McCaul and Williams, 1981). Rod-shaped SCV range from 0.2 to 0.5 μm in length and have a characteristic condensed chromatin. Pleomorphic large cell variants (LCV) can exceed 1 μm in length and contain a relaxed chromatin (McCaul and Williams, 1981). The kinetics of *C. burnetii* differentiation has been established in Vero host cells (Coleman et al., 2004). Following infection, SCV differentiate into LCV over a lag phase lasting approximately two days. LCV then replicate during an exponential phase lasting roughly four days. The onset of stationary phase signals transition of LCV to non-replicative SCV, with extended incubations (>2 weeks) resulting in vacuoles harboring nearly homogeneous SCV.

Replating assays using a Vero cell model of infection indicate non-replicative SCV and replicative LCV are equally infectious (Coleman, et al., 2004). However, claims of enhanced SCV environmental stability are conjecture as survival studies have not been conducted on purified cell forms. Moreover, no information exists on infectivity of SCV and LCV for macrophage host cells or laboratory animals, and the roles cell forms play in the pathophysiology of Q fever. Our gaps in knowledge of SCV/LCV biology are largely due to experimental constraints imposed by the organism's previous obligate intracellular nature. For example, the background of host RNA associated with intracellular growth confounds transcriptome experiments to elucidate the *C. burnetii* gene expression program that governs development. Moreover, preparations of *C. burnetii* fractionated from host cells contain contaminating host protein, which complicates proteome approaches to identifying proteins associated with the unique phenotypes and ultrastructures of SCV and LCV. Consequently, only a few cell-form specific markers have been identified in *C. burnetii* (Coleman et al., 2007, Heinzen, et al., 1999), with a small, highly basic DNA binding protein termed ScvA considered the gold standard marker of the SCV (Heinzen et al., 1996).

The recent advance of host cell-free (axenic) growth of *C. burnetii* in acidified citrate cysteine media (ACCM) (Omsland et al., 2011, Omsland et al., 2009) has enabled new investigative approaches and development of advanced genetic tools (Beare et al., 2012, Beare et al., 2011). In the current study, we investigated whether *C. burnetii* developmental

transitions in host cells are reproduced during long-term cultivation in first and second generation ACCM (ACCM-1 and ACCM-2, respectively). ACCM-1 differs from ACCM-2 only by substitution of fetal bovine serum for methyl-β-cyclodextrin (Mβ-CD). We show that ACCM-2, but not ACCM-1, supports *C. burnetii* developmental transitions and long-term viability that are indistinguishable from host cell-grown organisms. Based on transcriptional profiling, failure of *C. burnetii* to transition to SCV and loss of viability in ACCM-1 is associated with significant upregulation of genes involved in defense against oxidative stress, suggesting Mβ-CD has an antioxidant effect in ACCM-2 that sustains *C. burnetii* viability and promotes normal developmental transitions.

2. Materials and methods

2.1. Cultivation of C. burnetii

The *C. burnetii* Nine Mile RSA439 (phase II, clone 4) strain was used in this study. Host cell propagation of bacteria was conducted using African green monkey kidney (Vero) fibroblasts (CCL-81; American Type Culture Collection) grown in RPMI medium (Invitrogen) supplemented with 2% (v/v) fetal bovine serum (FBS). Homogeneous SCV forms were purified from infected Vero cells at 21 to 28 days post-infection as previously described (Coleman, et al., 2004). The homogeneity of SCV was assessed by transmission electron microscopy (TEM) as previously described (Heinzen, et al., 1996).

For axenic cultivation, *C. burnetii* was grown in ACCM-1 and ACCM-2 prepared as previously described (Omsland, et al., 2011, Omsland, et al., 2009). Cultures were incubated at 37° C in a 2.5% O_2 and 5% CO_2 environment using a CO-170 incubator (New Brunswick Scientific, NJ). Oxygen was displaced by nitrogen gas.

2.2. Fluorescent focus-forming unit (FFU) and quantitative polymerase chain reaction (QPCR) assays

FFU and QPCR assays were conducted to enumerate infectivity and genome equivalents (GE), respectively. Twenty milliliters of ACCM-1 or ACCM-2 in T-75 flasks were inoculated with 1×10^6 GE ml^{-1} of *C. burnetii* SCV. Cultures were grown microaerobically and samples collected at the indicated times. For FFU assays, 500 μl samples were added to 500 μl of cell freezing media [RPMI supplemented with 10% DMSO (v/v) and 10% (v/v) FBS] in a 2 ml cryovial, then stored at −80°C. Thawed *C. burnetii* was serially diluted in serum-free RPMI, and 200 μl of inoculum applied in triplicate to confluent Vero cells in a 48-well tissue culture plate. Plates were centrifuged at 400 x *g* for 20 min, then the inocula aspirated and monolayers washed three times with phosphate-buffered saline (1.5 mM KH_2PO_4, 2.7 mM Na_2HPO_4-$7H_2O$, 155 mM NaCl, [pH 7.2]). Cells were overlayed with RPMI supplemented with 10% (v/v) FBS and incubated 5 days. Infected cells were fixed with cold 100% methanol and FFU stained by indirect immunofluorescence employing polyclonal rabbit antiserum generated against formalin-killed *C. burnetii*, and Alexa Fluor 448-conjugated goat anti-immunoglobulin G serum (Invitrogen). FFU were enumerated by fluorescence microscopy at 32X magnification using a Leitz Fluovert inverted microscope.

For QPCR assays, samples were collected at the indicated times, frozen at −80°C, and GE quantified using a *dotA* probe as previously described (Coleman, et al., 2004).

2.3. TEM

Twenty milliliters of ACCM-1 or ACCM-2 in T-75 flasks were inoculated with 1×10^6 GE ml^{-1} of *C. burnetii* SCV. Ten milliliter aliquots were removed at 4, 10, 14, and 21 days post-inoculation, then the bacteria were pelleted and processed for TEM as previously described (Omsland, et al., 2009).

2.4. Immunoblotting

C. burnetii was cultivated as described above for FFU and QPCR assays. At the indicated times, bacteria were collected and lysed in sodium dodecyl sulfate-polyacrylamide gel electrophoresis (SDS-PAGE) sample buffer [87.5 mM Tris-HCl (pH 6.8), 89.7 mM SDS, 350 mM β-mercaptoethanol, 38 μM bromophenol blue, 9% (v/v) glycerol] and boiled for 10 min. Proteins were separated on precast 4 to 20% gradient SDS-PAGE gels (Thermo Scientific) and transferred to a 0.45 μm PVDF membrane (Millipore). Membranes were blocked overnight at 4° C in Tris-buffered saline [TBS; 50 mM NaCl, 20 mM Tris-HCl, (pH 8.0)] containing 0.1% (v/v) Tween-20 and 3% nonfat milk (w/v) (TBST). Membranes were then incubated with anti-ScvA rabbit polyclonal antibody (Heinzen, et al., 1996), followed by anti-rabbit IgG secondary antibody conjugated to horseradish peroxidase (Pierce, Rockford, IL). Reacting protein was detected via enhanced chemiluminescence using ECL Pico reagent (Pierce) and CL-XPosure film (Pierce).

2.5. Transcription microarray analysis

Ten milliliters of ACCM-1 or ACCM-2 in T-75 flasks were inoculated with 1.0×10^6 GE ml^{-1} of *C. burnetii* in quadruplicate. Cultures were incubated for 14 days, then bacteria were pelleted from 8 mls of medium and lysed in 1 ml of Trizol reagent (Invitrogen). Samples frozen at −80° C and RNA was extracted as previously described (Virtaneva et al., 2005).

A MicrobEnrich kit (Applied Biosystems) was used to increase the relative level of *C. burnetii* RNA. Enriched RNA (~1 μg) was amplified using a MessageAmp II Bacteria kit (Applied Biosystems). Briefly, double stranded cDNA was synthesized and purified using a QiaQuick 96-well system. Biotin-labeled cRNA was then *in vitro* transcribed using cDNA as a template. Ten μg of labeled cRNA was fragmented using Ambion 10X fragmentation buffer (Invitrogen) and incubation at 75°C for 15 min. Samples were hybridized to a custom Affymetrix GeneChip (RMLchip3a520351F) that contain probes sets corresponding to >96% of the open reading frames encoded by Nine Mile RSA493 reference strain (Beare et al., 2009, Seshadri et al., 2003).

Hybridization, fluidics, and scanning were performed according to standard Affymetrix protocols (http://www.affymetrix.com). Command Console (CC v3.1, http://www.Affymetrix.com) software was used to convert the image files to cell intensity data (cel files). All cel files, representing individual samples, were normalized by using the trimmed mean scaling method within expression console (EC v1.2, http://www.Affymetrix.com) to produce the analyzed cel files (chp files) along with the report files. An ANOVA was performed within Partek (Partek, Inc. St. Louis, Mo., v6.6 6.12.0420) to obtain multiple test corrected *p*-values using the false discovery rate method (Tusher et al., 2001). Significance at the 0.05 level was used to filter the probe-set list. These data were combined with fold change values, signal confidence (above background), cross hybridization to mock, and call consistency (as a percent) as calculated using custom Excel templates for each comparison.

The microarray data have been deposited in the NCBI GEO public database under accession number GSE51135.

2.6. QuantiGene measurement of gene expression

Validation of microarray expression results was conducted using the QuantiGene 2.0 assay system (Affymetrix) and custom designed probes according to the manufacturer's directions (Panomics, Santa Clara, CA). cRNA (0.2 μg) used in the microarray experiment was diluted in QuantiGene lysis buffer and combined with blocking buffer and probes. RNA solutions were loaded into a 96-well capture plate and incubated for 24 h at 55° C. The remainder of

the assay was carried out according to manufacturer's protocol. RNA was detected by luminescence over 1000 ms with a Tecan Safire^2 microplate reader. Background luminescence was determined using a water (no cRNA) control sample and this value was subtracted from each cRNA sample. Transcriptional signals were normalized to *C. burnetii* GE, measured from a replicate sample by QPCR (Coleman, et al., 2004). QuantiGene assays were also conducted on independent samples. Bacteria from 1 ml of ACCM culture were pelleted, the supernatant removed, and the pellet lysed in 1 ml of QuantiGene lysis buffer. mRNA was assayed directly according to the manufacturer's protocol.

3. Results

3.1. Growth kinetics of C. burnetii in ACCM-1 and ACCM-2 are similar

To investigate the effects of long-term axenic cultivation of *C. burnetii* on growth and viability, bacteria were grown in ACCM-1 and ACCM-2 for 21 days. Samples were collected at 2, 4, 6, 8, 10, 12, 14 and 21 post-inoculation of media with SCV purified from Vero cells. Growth of *C. burnetii* was first assessed by measuring GE by QPCR. *C. burnetii* exhibited similar growth kinetics over 21 days in both media. Approximately 3 logs of growth occurred over the first 3 days of incubation, with no subsequent change in GE out to 21 days post-inoculation (Fig. 1).

To determine the degree to which *C. burnetii* genomes correlated with viability, parallel infectious FFU assays were conducted using bacteria collected at the same time points (Fig. 1). GE/FFU ratios averaged 97.0 (± 29.4) and 68.0 (± 18.2) through 10 days of growth in ACCM-1 and ACCM-2, respectively, indicating similar viability in each medium. These ratios are comparable to Vero cell-derived *C. burnetii* replated through an 8 day infection time course (Coleman, et al., 2004). Organisms cultivated in ACCM-2 retained a GE/FFU average of 62.08 (± 13.37) throughout the remainder of 21 day time course in ACCM-2, indicating no loss in viability. In stark contrast, *C. burnetii* grown in ACCM-1 showed a precipitous loss in viability with GE/FFU ratios of 104.9, 374.0, and 2,574,545.0 at 12, 14, and 21 days post-inoculation, respectively. In two separate experiments, no FFU were detected at 21 days (data not shown).

3.2 Only ACCM-2 supports LCV to SCV morphological transition

In infected Vero cells, stationary phase correlates with LCV transition to SCV that remain viable for at least 21 days post-infection (Coleman, et al., 2004). To determine whether axenic media supports morphological transitions, TEM was conducted on bacteria harvested after 4, 10, 14 and 21 days of growth in axenic media (Fig. 2). When compared to the SCV starting inoculum, nearly all bacteria in ACCM-1 and ACCM-2 showed obvious transition to LCV after 4 days of growth. At 10 days, bacteria in both media displayed a continuum of forms with a few SCV in the population. At 14 days, bacteria from ACCM-2 showed an increased percentage of SCV. However, bacteria from ACCM-1 had a disorganized appearance that, at 21 days, transitioned to bacteria with a ghost-like appearance containing condensed chromatin but otherwise devoid of cytoplasmic content. This contrasted markedly with *C. burnetii* cultured for 21 days in ACCM-2 that had a typical SCV appearance. Loss of viability and failed LCV to SCV transition in ACCM-1 was associated with no production of the SCV-specific protein, ScvA (Fig. 3).

3.3. Transcriptional profiling shows upregulation of genes associated with oxidative stress defense in ACCM-1

C. burnetii is remarkably resistant to chemical and physical treatments (Williams, 1991). For example, infectious bacteria can be recovered from dried guinea pig blood after 182 days (Williams, 1991) and after pressure treatment of 50,000 lb $(in^2)^{-1}$ (McCaul et al., 1991).

Thus, the dramatic decline in viability of *C. burnetii* in ACCM-1 is highly uncharacteristic of this hardy pathogen. To gain insight into the physiology associated with the ~ 6 log decrease in *C. burnetii* viability in ACCM-1 from day 14 to day 21, we characterized by microarray the transcriptional profiles of *C. burnetii* after 14 days of growth in ACCM-1 and ACCM-2.

Principal components analysis revealed greater separation between bacteria cultured in ACCM-1 and ACCM-2 than between replicates, thus producing a significant differentially expressed gene list between the two samples (Fig. 4A). Of the 1751 gene probe sets on the microarray, 1546 displayed a statistically significant signal when probed with cRNA from ACCM-1 or ACCM-2-cultivated *C. burnetii*. However, only 43 genes were differentially expressed by ≥ 3-fold. Within this set, 33 genes were upregulated >3 fold and 10 genes were downregulated >3 fold in *C. burnetii* propagated in ACCM-1 compared to ACCM-2 (Table 1 and Supplementary Table S1).

Of particular note was upregulation of the oxidative stress genes *oxyR* (CBU1476; up 3.0-fold), *ahpC2* (CBU1477; up 7.9-fold) and *aphD* (CBU1478; up 17.1-fold) by *C. burnetii* during growth in ACCM-1. *ahpC2D* resides in a predicted operon immediately downstream from *oxyR*, which is transcribed in the opposite direction (Beare, et al., 2009, Mao et al., 2009). OxyR is a LysR family transcriptional regulator that upregulates antioxidant genes in response to peroxide stress (Dubbs and Mongkolsuk, 2012). AhpC2 is a peroxiredoxin that pairs with the peroxiredoxin reductase AhpD (collectively termed an alkyl hydroperoxidase reductase) to detoxify hydrogen peroxide, organic hydroperoxides, and peroxynitrite (Mishra and Imlay, 2012, Steele et al., 2010). *C. burnetii ahpC2D* is predicted to reside within the *oxyR* regulon (Mishra and Imlay, 2012) and to serve a critical role in detoxifying peroxides because the pathogen lacks a functional catalase (Mertens and Samuel, 2012).

To validate microarray results, QuantiGene analysis of *oxyR*, *ahpC2*, and *ahpD* was conducted on the cRNA used in the microarray experiment. CBU0920, encoding a fatty acid desaturase, was included as control gene that was not differentially expressed by *C. burnetii* growing in the ACCM-1 or ACCM-2. QuantiGene measurements also showed significant upregulation of *oxyR*, *ahpC2*, and *ahpD by C. burnetii* growing in ACCM-1 (Fig. 4b). Variation in the degree of upregulation between microarray and QuantiGene data sets likely reflects differences in the dynamic range of each assay.

3.4 Viability of C. burnetii in ACCM-1 can be rescued with Mβ-CD and corresponds to down regulation of ahp genes

Upregulation of *oxyR*, *ahpC2*, and *ahpD* transcription by *C. burnetii* growing in ACCM-1 suggests the organism is experiencing elevated oxidative stress that may lead to failed LCV to SCV transition and pathogen death. Oxidants such as superoxide anion and hydrogen peroxide can arise endogenously from bacterial metabolism (e. g., respiration, oxidation of flavoenzymes), or exogenously from photochemical oxidation and/or auto-oxidation of media compounds (e. g., amino acids, fatty acids). Relative to ACCM-2, ACCM-1 contains FBS (1%), but lacks Mβ-CD (1 mg/ml). Thus, both of these compounds could be associated with media oxidant levels. As a rich nutrient source, FBS might short circuit the transition into stationary phase physiology with coincident accumulation of endogenously-derived oxidants. Alternately, FBS could contain nutrients that generate peroxides upon oxidation, such as free fatty acids. However, the growth kinetics and viability of *C. burnetii* cultivated in ACCM-2 supplemented with FBS were indistinguishable from organisms grown in ACCM-2 alone (data not shown). This result suggested that Mβ-CD serves a protective anti-oxidant role. To probe this possibility, Mβ-CD (1 mg/ml) was added to ACCM-1 at 7 days post-inoculation and *ahpC2* and *ahpD* expression measured at 14 days post-inoculation. *C. burnetii* viability was also examined at 21 days post-inoculation. Mβ-CD supplementation

inoculation rescued approximately 6 logs of growth (Fig. 5A) and resulted in 3.8- and 5.6-fold decreased expression of *ahpC2* and *ahpD*, respectively (Fig. 5B).

4. Discussion

In the current study, we demonstrate that growth kinetics, developmental transitions and long-term viability of *C. burnetii* axenically grown in ACCM-2 are similar to bacteria propagated in mammalian host cells. Both ACCM-1 and ACCM-2 support differentiation of SCV to LCV during log phase growth, but only ACCM-2 supports differentiation of LCV to SCV during stationary phase. Lack of LCV to SCV differentiation in ACCM-1 is associated with a near total loss in viability and the appearance of ghost-like bacteria that appear to be primarily comprised of cell envelope and compacted chromatin. Because these non-viable bacteria retain their genome during stationary phase death, GE-based growth curves of *C. burnetii* cultivated in ACCM-1 and ACCM-2 are similar.

Transcriptional profiling reveals the oxidative stress genes *oxyR*, *ahpC2*, and *ahpD* are significantly upregulated by *C. burnetii* during growth in ACCM-1 relative to growth in ACCM-2. OxyR is specifically activated by various peroxides (Dubbs and Mongkolsuk, 2012) and regulates expression of AhpC2 and AhpD that detoxify these molecules (Mishra and Imlay, 2012, Steele, et al., 2010). Addition of Mβ-CD (a unique ingredient of ACCM-2) to ACCM-1 at 7 days post-inoculation rescues viability of *C. burnetii* to near that of bacteria cultivated in ACCM-2 and results in down-regulation of *ahpC2* and *ahpD*. These results suggest that deficient growth and development in ACCM-1 is at least partly due to elevated peroxide stress, and that Mβ-CD serves to defend *C. burnetii* against this insult.

Susceptibility to oxidants may be the Achilles' heel of *C. burnetii*. Host cell-free organisms are roughly 100 times more sensitive to hydrogen peroxide than *Escherichia coli* (A. Omsland and R. A. Heinzen, unpublished data). Interestingly, several virulent strains of *C. burnetii*, such as the Nine Mile reference strain, lack catalase in the form of monofunctional heme catalase (KatE) (Mertens and Samuel, 2012). Therefore, these strains must rely on peroxidases, such as AhpC2, to scavenge hydrogen peroxide. The AhpC class of peroxiredoxins appears specifically equipped for detoxification of low levels of endogenous hydrogen peroxide produced by respiratory metabolism (Mishra and Imlay, 2012, Steele, et al., 2010). Conversely, catalase is better designed to deal with high levels of hydrogen peroxide, as would be encountered during a phagocyte oxidative burst (Mishra and Imlay, 2012). *C. burnetii* secretes an acid phosphatase (Acp, CBU0335) that inhibits phagocyte NADPH oxidase. Thus, the bacterium can avoid the rapid release of phagocyte-derived superoxide anion and hydrogen peroxide following infection, thereby decreasing the need for catalase during intracellular growth (Hill and Samuel, 2011, Siemsen et al., 2009). Microaerophilic metabolism by *C. burnetii* is another adaptation that lessens oxidative stress. The sensitivity of *C. burnetii* to oxidative death has implications for laboratory and field decontamination treatments.

How Mβ-CD protects *C. burnetii* from oxidative stress and maintains viability is unclear. Cyclodextrins are cyclic oligosaccharides consisting of 6 to 8 glucose moieties. They have a polar surface and hydrophobic core, and are extensively employed in industry and pharmaceuticals to solubilize a wide array of hydrophobic molecules (Del Valle, 2004). As media supplements, cyclodextrins also promote growth of the fastidious pathogenic bacteria *Helicobacter pylori* (Marchini et al., 1995) and *Bordetella pertussis* (Imaizumi et al., 1983), presumably by their ability to sequester auto-inhibitory hydrophobic metabolites, such as certain fatty acids that are released during bacterial growth (Frohlich et al., 1996, Imaizumi, et al., 1983, Miller et al., 1977). ACCM-1 and ACCM-2 are supplemented with L-cysteine to account for *C. burnetii* auxotrophy. However, a supraphysiologic concentration (1.5 mM)

is needed (Omsland, et al., 2009), possibly because L-cysteine is easily oxidized to the dipeptide L-cystine, which the bacterium cannot transport (Ewann and Hoffman, 2006). Oxidation of L-cysteine also produces hydrogen peroxide (Hoffman et al., 1983) that may in turn oxidize hydrophobic media constituents that are sequestered by Mβ-CD and made unavailable for redox chemistry with *C. burnetii* (Del Valle, 2004). Analysis of cyclodextrin complexes purified from culture supernatants might identify toxic media components (Saito et al., 2012).

As demonstrated here and elsewhere (Coleman, et al., 2004, Omsland, et al., 2009), *C. burnetii* developmental forms are roughly equally infectious for Vero cells based on GE/FFU ratios (Coleman, et al., 2004). This behavior is unlike that of cell forms generated during biphasic development of *Chlamydia spp*. (Abdelrahman and Belland, 2005) and *Legionella pneumophila* (Molofsky and Swanson, 2004), where one developmental form is specifically adapted for infection. Developmental transitions of *C. burnetii* appear unrelated to infectivity, at least for cultured cells. Whether equal infectivity extends to animal models of infection is unknown.

Pronounced extracellular stability of *C. burnetii* is clearly important in the epidemiology of Q fever. SCV structural attributes, such as compacted chromatin and resistance to physical disruption (Amano et al., 1984, McCaul, et al., 1991, McCaul, et al., 1981), led to the hypothesis that the SCV is better adapted for extracellular survival, and consequently, responsible for most natural infections (Heinzen, et al., 1999). However, direct evidence supporting differential resistance to environmental stressors by cell forms, such as desiccation and ultraviolet light, is lacking. The similarity of *C. burnetii* biphasic development in ACCM-2 and mammalian host cells now provides an amenable experimental system to probe the biological characteristics of SCV and LCV. Furthermore, the environmental signals and gene expression that drive development can now be defined without complications associated with host cell background.

Supplementary Material

Refer to Web version on PubMed Central for supplementary material.

Acknowledgments

We thank Anders Omsland for critical review of the manuscript. This work was supported by the Intramural Research Program of the National Institutes of Health, National Institute of Allergy and Infectious Diseases

References

Abdelrahman YM, Belland RJ. The chlamydial developmental cycle. FEMS Microbiol Rev. 2005; 29:949–959. [PubMed: 16043254]

Amano K, Williams JC, McCaul TF, Peacock MG. Biochemical and immunological properties of *Coxiella burnetii* cell wall and peptidoglycan-protein complex fractions. J Bacteriol. 1984; 160:982–988. [PubMed: 6501233]

Beare PA, Larson CL, Gilk SD, Heinzen RA. Two systems for targeted gene deletion in *Coxiella burnetii*. Appl Environ Microbiol. 2012; 78:4580–4589. [PubMed: 22522687]

Beare PA, Sandoz KM, Omsland A, Rockey DD, Heinzen RA. Advances in genetic manipulation of obligate intracellular bacterial pathogens. Front Microbiol. 2011; 2:97. [PubMed: 21833334]

Beare PA, Unsworth N, Andoh M, Voth DE, Omsland A, Gilk SD, Williams KP, Sobral BW, Kupko JJ 3rd, Porcella SF, Samuel JE, Heinzen RA. Comparative genomics reveal extensive transposon-mediated genomic plasticity and diversity among potential effector proteins within the genus *Coxiella*. Infect Immun. 2009; 77:642–656. [PubMed: 19047403]

Coleman SA, Fischer ER, Cockrell DC, Voth DE, Howe D, Mead DJ, Samuel JE, Heinzen RA. Proteome and antigen profiling of *Coxiella burnetii* developmental forms. Infect Immun. 2007; 75:290–298. [PubMed: 17088354]

Coleman SA, Fischer ER, Howe D, Mead DJ, Heinzen RA. Temporal analysis of *Coxiella burnetii* morphological differentiation. J Bacteriol. 2004; 186:7344–7352. [PubMed: 15489446]

Del Valle EMM. Cyclodextrins and their uses: a review. Process Biochemistry. 2004; 39:1033–1046.

Dubbs JM, Mongkolsuk S. Peroxide-sensing transcriptional regulators in bacteria. J Bacteriol. 2012; 194:5495–5503. [PubMed: 22797754]

Ewann F, Hoffman PS. Cysteine metabolism in *Legionella pneumophila*: characterization of an L-cystine-utilizing mutant. Appl Environ Microbiol. 2006; 72:3993–4000. [PubMed: 16751507]

Frohlich BT, d'Alarcao M, Feldberg RS, Nicholson ML, Siber GR, Swartz RW. Formation and cell-medium partitioning of autoinhibitory free fatty acids and cyclodextrin's effect in the cultivation of *Bordetella pertussis*. J Biotechnol. 1996; 45:137–148. [PubMed: 9147447]

Heinzen RA, Hackstadt T, Samuel JE. Developmental biology of *Coxiella burnettii*. Trends Microbiol. 1999; 7:149–154. [PubMed: 10217829]

Heinzen RA, Howe D, Mallavia LP, Rockey DD, Hackstadt T. Developmentally regulated synthesis of an unusually small, basic peptide by *Coxiella burnetii*. Mol Microbiol. 1996; 22:9–19. [PubMed: 8899704]

Hill J, Samuel JE. *Coxiella burnetii* acid phosphatase inhibits the release of reactive oxygen intermediates in polymorphonuclear leukocytes. Infect Immun. 2011; 79:414–420. [PubMed: 21078859]

Hoffman PS, Pine L, Bell S. Production of superoxide and hydrogen peroxide in medium used to culture *Legionella pneumophila*: catalytic decomposition by charcoal. Appl Environ Microbiol. 1983; 45:784–791. [PubMed: 6303219]

Huijsmans CJ, Schellekens JJ, Wever PC, Toman R, Savelkoul PH, Janse I, Hermans MH. Single-nucleotide-polymorphism genotyping of *Coxiella burnetii* during a Q fever outbreak in The Netherlands. Appl Environ Microbiol. 2011; 77:2051–2057. [PubMed: 21257816]

Imaizumi A, Suzuki Y, Ono S, Sato H, Sato Y. Heptakis(2,6-O-dimethyl)beta-cyclodextrin: a novel growth stimulant for *Bordetella pertussis* phase I. J. Clin. Microbiol. 1983; 17:781–786.

Mao F, Dam P, Chou J, Olman V, Xu Y. DOOR: a database for prokaryotic operons. Nucleic Acids Res. 2009; 37:D459–463. [PubMed: 18988623]

Marchini A, d'Apolito M, Massari P, Atzeni M, Copass M, Olivieri R. Cyclodextrins for growth of *Helicobacter pylori* and production of vacuolating cytotoxin. Arch Microbiol. 1995; 164:290–293. [PubMed: 7487335]

McCaul TF, Banerjee-Bhatnagar N, Williams JC. Antigenic differences between *Coxiella burnetii* cells revealed by postembedding immunoelectron microscopy and immunoblotting. Infect Immun. 1991; 59:3243–3253. [PubMed: 1715326]

McCaul, TF.; Hackstadt, T.; Williams, JC. Ultrastructural and biological aspects of *Coxiella burnetii* under physical disruptions. In: Burgdorfer, W.; Anacker, RL., editors. Rickettsiae and Rickettsial Diseases. Academic Press; New York: 1981. p. 267-280.

McCaul TF, Williams JC. Developmental cycle of *Coxiella burnetii*: structure and morphogenesis of vegetative and sporogenic differentiations. J Bacteriol. 1981; 147:1063–1076. [PubMed: 7275931]

Mertens K, Samuel JE. Defense mechanisms against oxidative stress in *Coxiella burnetii*: adaptation to a unique intracellular niche. Adv Exp Med Biol. 2012; 984:39–63. [PubMed: 22711626]

Miller RD, Brown KE, Morse SA. Inhibitory action of fatty acids on the growth of *Neisseria gonorrhoeae*. Infect Immun. 1977; 17:303–312. [PubMed: 19358]

Mishra S, Imlay J. Why do bacteria use so many enzymes to scavenge hydrogen peroxide? Arch Biochem Biophys. 2012; 525:145–160. [PubMed: 22609271]

Molofsky AB, Swanson MS. Differentiate to thrive: lessons from the *Legionella pneumophila* life cycle. Mol Microbiol. 2004; 53:29–40. [PubMed: 15225301]

Omsland A, Beare PA, Hill J, Cockrell DC, Howe D, Hansen B, Samuel JE, Heinzen RA. Isolation from animal tissue and genetic transformation of *Coxiella burnetii* are facilitated by an improved axenic growth medium. Appl Environ Microbiol. 2011; 77:3720–3725. [PubMed: 21478315]

Omsland A, Cockrell DC, Howe D, Fischer ER, Virtaneva K, Sturdevant DE, Porcella SF, Heinzen RA. Host cell-free growth of the Q fever bacterium *Coxiella burnetii*. Proc Natl Acad Sci USA. 2009; 106:4430–4434. [PubMed: 19246385]

Roest HI, Tilburg JJ, van der Hoek W, Vellema P, van Zijderveld FG, Klaassen CH, Raoult D. The Q fever epidemic in The Netherlands: history, onset, response and reflection. Epidemiol Infect. 2011; 139:1–12. [PubMed: 20920383]

Saito N, Ishida Y, Seno K, Hayashi F. Methyl-beta-cyclodextrin is a useful compound for extraction and purification of prenylated enzymes from the retinal disc membrane. Protein Expr Purif. 2012; 82:168–173. [PubMed: 22226869]

Seshadri R, Paulsen IT, Eisen JA, Read TD, Nelson KE, Nelson WC, Ward NL, Tettelin H, Davidsen TM, Beanan MJ, Deboy RT, Daugherty SC, Brinkac LM, Madupu R, Dodson RJ, Khouri HM, Lee KH, Carty HA, Scanlan D, Heinzen RA, Thompson HA, Samuel JE, Fraser CM, Heidelberg JF. Complete genome sequence of the Q-fever pathogen *Coxiella burnetii*. Proc Natl Acad Sci USA. 2003; 100:5455–5460. [PubMed: 12704232]

Siemsen DW, Kirpotina LN, Jutila MA, Quinn MT. Inhibition of the human neutrophil NADPH oxidase by *Coxiella burnetii*. Microbes Infect. 2009; 11:671–679. [PubMed: 19379824]

Steele KH, Baumgartner JE, Valderas MW, Roop RM 2nd. Comparative study of the roles of AhpC and KatE as respiratory antioxidants in *Brucella abortus* 2308. J Bacteriol. 2010; 192:4912–4922. [PubMed: 20675478]

Tissot-Dupont H, Amadei MA, Nezri M, Raoult D. Wind in November, Q fever in December. Emerg Infect Dis. 2004; 10:1264–1269. [PubMed: 15324547]

Tusher VG, Tibshirani R, Chu G. Significance analysis of microarrays applied to the ionizing radiation response. Proc Natl Acad Sci USA. 2001; 98:5116–5121. [PubMed: 11309499]

Virtaneva K, Porcella SF, Graham MR, Ireland RM, Johnson CA, Ricklefs SM, Babar I, Parkins LD, Romero RA, Corn GJ, Gardner DJ, Bailey JR, Parnell MJ, Musser JM. Longitudinal analysis of the group A Streptococcus transcriptome in experimental pharyngitis in cynomolgus macaques. Proc Natl Acad Sci USA. 2005; 102:9014–9019. [PubMed: 15956184]

Voth DE, Heinzen RA. Lounging in a lysosome: the intracellular lifestyle of *Coxiella burnetii*. Cell Microbiol. 2007; 9:829–840. [PubMed: 17381428]

Williams, JC. Infectivity, virulence, and pathogenicity of *Coxiella burnetii* for various hosts. In: Williams, JC.; Thompson, HA., editors. Q fever: The biology of *Coxiella burnetii*. CRC Press, Inc; Boca Raton, FL: 1991. p. 21-71.

Highlights

- Long-term viability and developmental transitions of *Coxiella burnetii* were examined in axenic media.
- The axenic medium ACCM-2 supports viability and developmental transitions.
- Loss of viability in ACCM-1 is associated with failed development transition.
- *Coxiella* growing in ACCM-1 experiences elevated oxidative stress.
- Axenic growth in ACCM-2 is an amenable system for studying the molecular biology of *Coxiella* biphasic development.

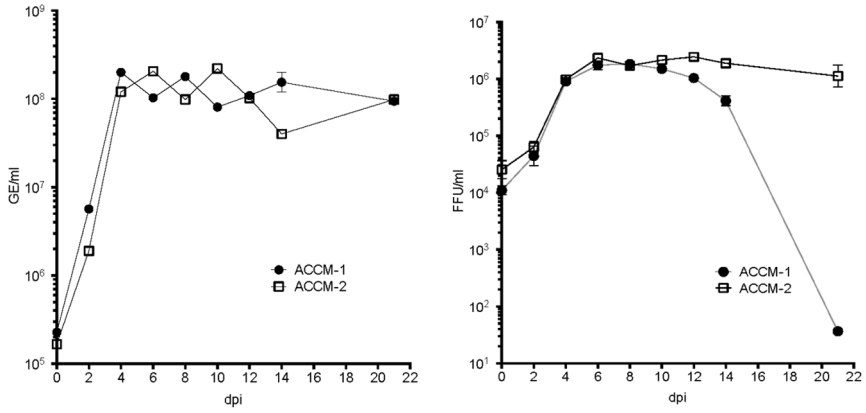

Figure 1.

ACCM-2 supports long-term viability of *C. burnetii*. Quantitation of *C. burnetii* genome equivalents (GE) (right) and infectious focus-forming units (FFU) (left) and over a 21 day time course of growth in ACCM-1 and ACCM-2. The results shown are from one experiment performed in triplicate and are representative of three independent experiments. Error bars indicate the standard errors of the means.

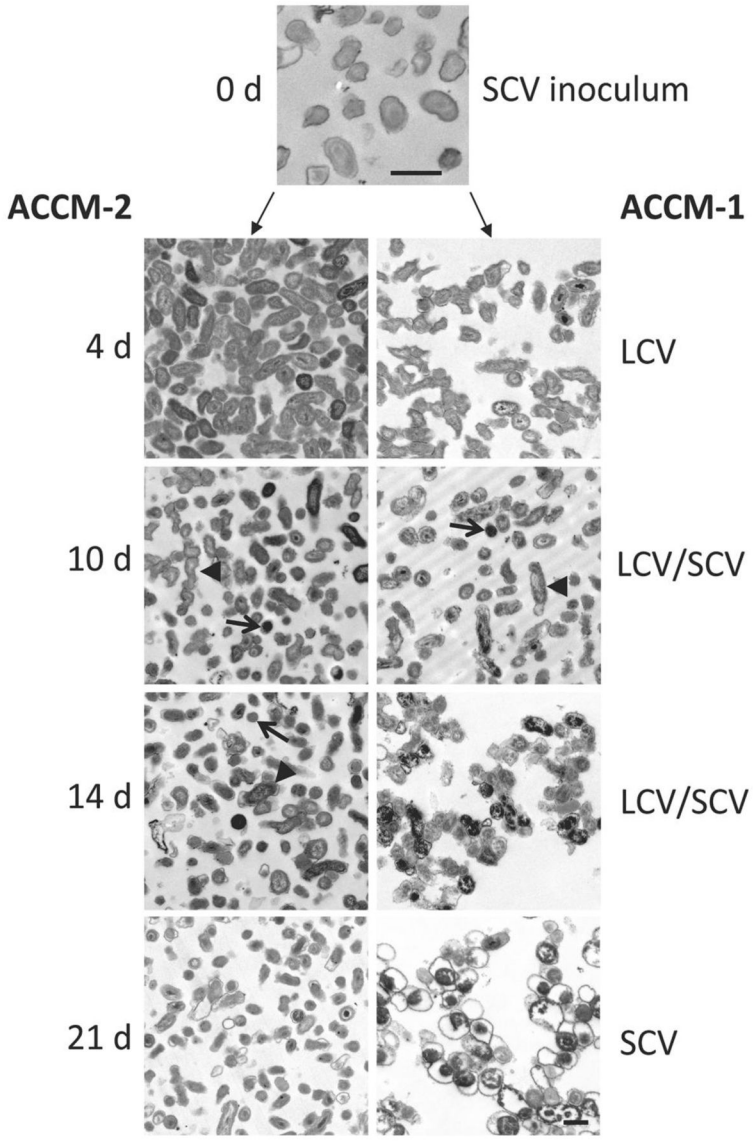

Figure 2.
ACCM-2 supports *C. burnetii* developmental transitions. Electron micrographs of *C. burnetii* grown in ACCM-1 and ACCM-2 for 4, 10, 14, and 21 days, and the SCV inoculum derived from Vero cells. Arrows and arrowheads designate representative LCV and SCV, respectively. Scale bar, 0.5 μM.

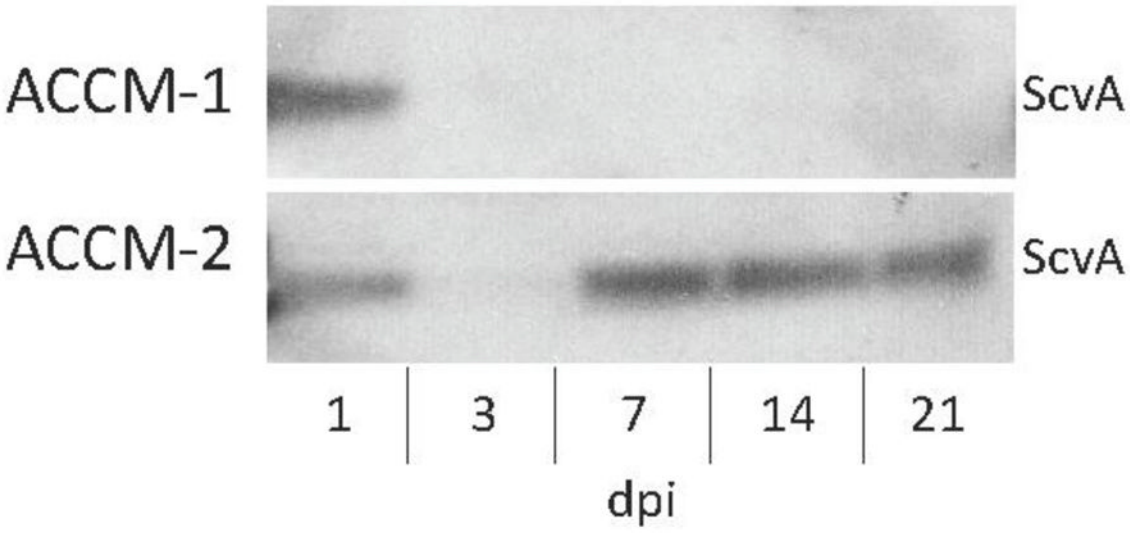

Figure 3.

C. burnetii cultivated in ACCM-1 fails to synthesize ScvA during log to stationary phase transition. *C. burnetii* was collected after 1, 3, 7, 14, and 21 days of growth in ACCM-1 and ACCM-2, then analyzed by immunoblotting for the presence of SCV marker protein, ScvA (3.6 kDa). Each lane was loaded with 1×10^6 GE of *C. burnetii.*

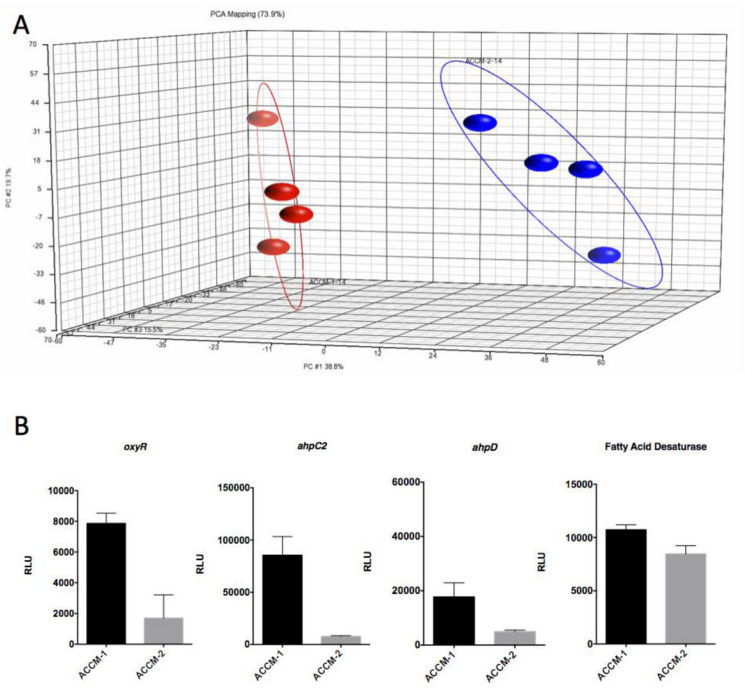

Figure 4.

Transcriptional profiling shows elevated transcription of oxidative stress genes by *C. burnetii* during growth in ACCM-1. *C. burnetii* gene expression profiles were assessed by microarray following replication for 14 days in ACCM-1 and ACCM-2. (A) Principal-component analysis of 4 replicate samples showing distinct grouping of ACCM-1 (red) and ACCM-2-cultivated (blue) *C. burnetii*. (B) QuantiGene verification of *oxyR* (CBU1476), *ahpC2* (CBU1477), *ahpD* (CBU1478), and CBU0920, encoding a fatty acid desaturase. Expression is shown as relative light units (RLU). Error bars indicate the standard errors of the mean of three independent experiments, each done in triplicate.

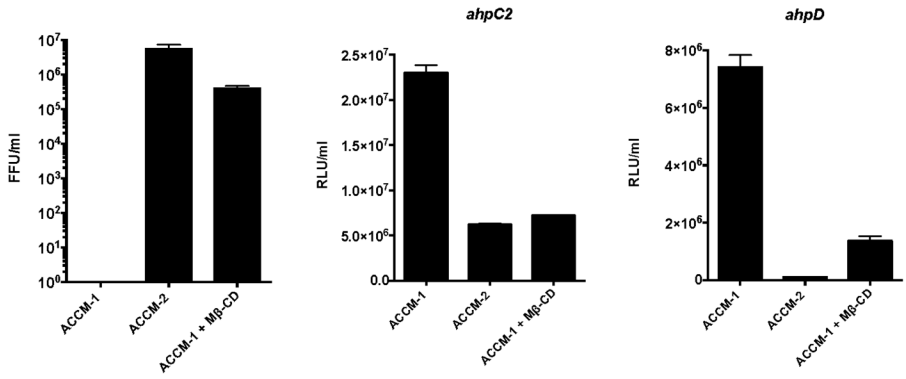

Figure 5.

Supplementation of ACCM-1 with Mβ-CD rescues viability of *C. burnetii* and lowers expression of oxidative stress genes. (A) Quantitation of *C. burnetii* infectious focus-forming units (FFU) at 21 days post-inoculation of ACCM-1, ACCM-2, or ACCM-1 supplemented with Mβ-CD (1 mg/ml) at 7 days post-inoculation. The results shown are from one experiment performed in triplicate and are representative of three independent experiments. Error bars indicate the standard errors of the means. (B) QuantiGene measurement of expression of *ahpC2* and (C) *ahpD* by *C. burnetii* at 14 days post-inoculation of ACCM-1, ACCM-2, or ACCM-1 supplemented with Mβ-CD (1 mg/ml) at 7 days post-inoculation. Expression is shown as relative light units (RLU). Error bars indicate the standard errors of the mean of three independent experiments, each done in triplicate.

Table 1

Genes up or downregulated ≥ 3-fold by *C. burnetii* after 14 days of growth in ACCM-1 as compared to growth in ACCM-2.

CBU No.	Function	Gene	ACCM-2 signal	ACCM-1 signal	Fold change
CBU0926	3-hydroxyisobutyrate dehydrogenase	*mmsB*	6,712	1,565	−4.29
CBU1847	hypothetical protein		4,056	1,053	−3.85
CBU0956	hypothetical protein		10,987	2,860	−3.84
CBU1078	hypothetical protein		3,136	896	−3.50
CBU2021	ATPase		2,259	673	−3.36
CBU0893	acetyl-coA carboxylase carboxyl transferase subunit beta	*accD*	3,708	1,150	−3.22
CBU0909	sua5/YciO/YrdC/YwlC family protein		4,330	1,365	−3.17
CBU0480	arginine repressor ArgR	*argR*	7,601	2,463	−3.09
CBU1266	lipoyl synthase	*lipA*	1,128	370	−3.05
CBU0716	thioredoxin reductase		4,238	1,395	−3.04
CBU0831	asparagine synthetase	*asnB-1*		326	3.05
CBU1188	seryl-tRNA synthetase	*serS*	86	230	3.65
CBU1629	IcmL	*icmL.1*	400	1,200	3.63
CBU1476	hydrogen peroxide-inducible genes activator	*oxyR*	1,688	5,122	3.03
CBU1632	IcmO	*icmO*	575	1,763	3.06
CBU1465	hypothetical protein		699	2,145	3.07
CBU1930a	hypothetical protein		1,297	4,030	3.11
CBU1625	hypothetical protein	*icmC*	314	995	3.16
CBU1469	rod shape-determining protein	*mreD*	504	1,597	3.17
CBURNA046	23S rRNA		13,591	43,479	3.20
CBU1471	rod shape-determining protein MreB	*mreB*	1,099	3,695	3.36
CBU1348	hypothetical protein		128	460	3.49
CBU0745	ribosome-associated factor Y		1,081	3,916	3.62
CBU1474	aspartyl/glutamyl-tRNA amidotransferase subunit A	*gatA*	162	601	4.06
CBU1412	hypothetical protein		278	1,043	3.76
CBU1626	hypothetical protein	*icmG*	395	1,514	3.84
CBU0259	hypothetical protein		551	2,135	3.87
CBU1458a	hypothetical protein		197	772	3.92
CBU1628	IcmK	*icmK*	535	2,172	4.06

CBU No.	Function	Gene	ACCM-2 signal	ACCM-1 signal	Fold change
CBU0304	endoribonuclease L-PSP		1,297	5,441	4.19
CBU0311	hypothetical protein		399	1,923	4.82
CBU1479	hypothetical protein		140	674	4.83
CBU1470	rod shape-determining protein MreC	*mreC*	189	942	4.97
CBU1472	hypothetical protein			1,249	5.93
CBU0596a	hypothetical protein		414	2,078	8.29
CBU1627	IcmE	*icmE*	155	799	5.16
CBU1475	aspartyl/glutamyl-tRNA amidotransferase subunit B	*gatB*	164	896	5.46
CBU1547	thymidylate synthase	*thyA*	227	1,299	5.72
CBU1477	peroxiredoxin	*ahpC2*	4,186	32,907	7.86
CBU1931	hypothetical protein		142	1,258	8.84
CBU0083	hypothetical protein		316	2,825	8.95
CBU1473	glutamyl/aspartyl-tRNA amidotransferase subunit C	*gatC*	223	2,050	9.20
CBU1478	peroxiredoxin reductase	*ahpD*	210	3,787	17.99